JOURNAL OF BACTERIOLOGY, Nov. 1995, p. 6560–6567 Vol. 177, No. 22
0021-9193/95/$04.00+0

Inhibition of Translation Initiation on *Escherichia coli gnd* mRNA by Formation of a Long-Range Secondary Structure Involving the Ribosome Binding Site and the Internal Complementary Sequence

JINGHUA TSAI CHANG,† CRISTINA BARTHEL-ROSA GREEN, AND RICHARD E. WOLF, JR.*

Department of Biological Sciences, University of Maryland Baltimore County, Baltimore, Maryland 21228

Received 5 July 1995/Accepted 12 September 1995

Previous research has indicated that the growth rate-dependent regulation of *Escherichia coli gnd* expression involves the internal complementary sequence (ICS), a negative control site that lies within the 6-phosphogluconate dehydrogenase coding sequence. To determine whether the ICS acts as a transcriptional operator or attenuator, we measured β-galactosidase-specific activities in strains carrying *gnd-lac* operon and protein fusions containing or lacking the ICS. Whereas the presence of the ICS repressed β-galactosidase expression from a protein fusion by 5-fold during growth on acetate and by 2.5-fold during growth on glucose, it had no effect on β-galactosidase expression from an operon fusion. In vitro ribosome binding experiments employing the primer extension inhibition (toeprint) assay demonstrated that the presence of the ICS in *gnd* mRNA reduces both the maximum extent and the rate of ternary complex formation. Moreover, the effects of deletions scanning the ICS on in vivo gene expression were highly correlated with the effects of the deletions on ribosome binding in vitro. In addition, the distal end of the ICS element was found to contribute more to ICS function than did the proximal portion, which contains the complement to the Shine-Dalgarno sequence. Finally, RNA structure mapping experiments indicated that the presence of the ICS in *gnd* mRNA reduces the access of the nucleotides of the ribosome binding site to the single-strand-specific chemical reagents dimethyl sulfate and kethoxal. Taken together, these data support the hypothesis that the role of the ICS in the growth rate-dependent regulation of *gnd* expression is to sequester the translation initiation region into a long-range mRNA secondary structure that blocks ribosome binding and thereby reduces the frequency of translation initiation.

Growth rate-dependent regulation is a fundamental genetic regulatory process that coordinates global gene expression with the nutritional quality of a cell's environment. As a model system for growth rate-dependent regulation of nonribosomal genes, we have been investigating the *Escherichia coli gnd* gene, which encodes 6-phosphogluconate dehydrogenase (6PGD; EC 1.1.1.44), an enzyme of the pentose phosphate pathway of central carbon metabolism. In *E. coli* K-12, the specific activity of 6PGD increases about threefold over the fourfold range of growth rates obtained with cells growing in minimal media with various carbon sources, e.g., acetate, in which the doubling time is about 4 h, and glucose, in which the doubling time is about 1 h (25). Antibody neutralization experiments demonstrated that this increase is due to an increase in the amount of 6PGD relative to total protein rather than to an increase in the activity of 6PGD molecules (25). Moreover, since reducing the growth rate by limiting the rate of glucose uptake decreased the amount of 6PGD, *gnd* gene expression is regulated by the cellular growth rate, not by the specific carbon source (25).

Much of the information regarding the mechanism of growth rate control of *gnd* expression has come from the properties of strains carrying *gnd-lac* operon and protein fusions (1, 2, 5). For example, the level of β-galactosidase does not increase with an increase in growth rate in strains carrying operon fusions prepared with phage MudI and located within the *gnd* gene at its normal chromosomal location (1). This led to the hypothesis that growth rate control is exerted on a posttranscriptional step in *gnd* expression, most likely translation but possibly mRNA stability, as well as on transcription (1).

The involvement of a negative control site located within the 6PGD coding sequence in the growth rate-dependent regulation of *gnd* expression was initially revealed by the phenotypes conferred by *gnd-lacZ* protein fusions prepared with phage MudII and located within the normal *gnd* gene (2). With all but one protein fusion strain, the level of β-galactosidase increased threefold with increasing growth rate, just like the growth rate dependence of the 6PGD level in a wild-type strain. In the remaining fusion, which had the smallest amount of the *gnd* structural gene fused to *lacZ*, the level of β-galactosidase was elevated threefold when the strain was grown on acetate, and it increased only slightly during growth on glucose (2). Subsequently, we carried out a genetic analysis using protein fusions carried on a λ prophage at *att*λ and identified the internal regulatory region as the segment of *gnd* mRNA lying between codons 71 and 74 (5). The sequence of this region is perfectly conserved in *Salmonella typhimurium* LT-2 and in other *E. coli* strains from natural populations (3, 4). We named this site the internal complementary sequence (ICS) because it is complementary to the Shine-Dalgarno sequence and surrounding nucleotides in the *gnd* mRNA leader, and we proposed that its negative control function is to sequester the *gnd* ribosome binding site (RBS) into a long-range mRNA secondary structure that blocks translation initiation (4, 5). To account for the growth rate-dependent regulation of the 6PGD level, we fur-

* Corresponding author. Mailing address: Department of Biological Sciences, University of Maryland Baltimore County, Baltimore, MD 21228. Phone: (410) 455-2268. Fax: (410) 455-3875. Electronic mail address: wolf@umbc.edu.

† Present address: Department of Ophthalmology, Johns Hopkins University School of Medicine, Baltimore, MD 21205.

ther proposed that the rate of formation or the stability of the secondary structure formed between the RBS and the ICS would vary with the growth rate and thus lead to a growth rate-dependent increase in either the stability or the translation efficiency of *gnd* mRNA (5). However, although the logic of these arguments is sound, the connection between the posttranscriptional regulation revealed by the properties of the operon fusions and the negative control revealed by the properties of the protein fusions has never been made. Thus, it may be only coincidental that the negative control site is complementary to the RBS. Moreover, even if the RBS-ICS secondary structure could be shown to form, it might mediate growth rate-dependent regulation by serving as a transcription attenuator. In fact, since this putative posttranscriptional regulation was uncovered before the ICS was discovered, it is not known whether the phage MudI-induced operon fusions contain or lack the ICS (1, 2). Accordingly, the ICS could also be an operator for the binding of a transcriptional repressor.

By direct measurement of the effect of growth rate on the abundance and half-life of *gnd* mRNA, Pease and Wolf (16) showed that the amount of *gnd* mRNA relative to total mRNA increases about 2.5-fold with an increasing growth rate and that the half-life of *gnd* mRNA does not change with changes in growth rate (16). They then showed mathematically that although the growth rate-dependent increase in 6PGD mass appears to be fully accounted for by a growth rate-dependent increase in *gnd* transcription, the increase in 6PGD mass requires that the translation efficiency of *gnd* mRNA increase with an increasing growth rate like that of the average mRNA. Moreover, after pointing out that the translation efficiency of *gnd* mRNA (and average mRNA) increases about threefold with an increasing growth rate, Pease and Wolf (16) argued that the ICS could serve the function of making the translation efficiency of *gnd* mRNA like that of the average mRNA; that is, without the ICS, the translation efficiency of *gnd* mRNA under slow-growth conditions would be elevated threefold and would not increase with an increasing growth rate. They also pointed out that the ICS could serve the alternative or the additional function of making the half-life of *gnd* mRNA independent of growth rate, as is the half-life of total mRNA; in this case, without the ICS, the half-life of *gnd* mRNA under slow-growth conditions would be threefold longer and decrease with an increasing growth rate.

In this report, we address several of the issues raised above. First, by comparing the effects of the ICS in *gnd-lac* operon and protein fusion strains, we rule out transcriptional repression or termination as the primary mechanism of action of the ICS and thus provide additional evidence that the ICS functions posttranscriptionally. Second, with in vitro "toeprint assays" (7), we show that the presence of the ICS in *gnd* mRNA reduces the maximum extent and the initial rate of formation of the translation initiation ternary complex and thus demonstrate directly that the ICS can block translation initiation, as originally proposed (4, 5). Moreover, we have prepared a set of in-frame deletions scanning the ICS and found a high correlation between the effects of the mutations on gene expression in vivo and their effects on ribosome binding in vitro, from which we argue that the primary regulatory function of the ICS is to inhibit translation initiation. Finally, by showing that the presence of the ICS in *gnd* mRNA reduces the accessibility of the nucleotides of the RBS to attack by single-strand-specific chemical reagents, we provide evidence for the capacity of *gnd* mRNA to form a long-range RBS-ICS secondary structure.

MATERIALS AND METHODS

Strains, plasmids, and phages. The strains used in this study are derivatives of *E. coli* K-12 strain W3110. The *gnd-lac* protein and operon fusions are named according to the *gnd* codon number at the *gnd-lac* fusion joint; the additional designations P and O refer to protein and operon fusions, respectively, while the designations (−) and (+) are used to specify whether the fusion is ICS^- or ICS^+, respectively. Thus, fusions CMP40(−) and CMP69(−) are protein fusions that lack the ICS and have 40 and 69 *gnd* codons, respectively, fused to *lacZ*. Fusions CMP40(+) and CMP69(+) are protein fusions that carry the 16-bp core ICS element (5′-CATCCTGTTAATGGTG-3′); fusion CMP78(+) carries the native ICS element (5). All of the fusions used for in vivo studies of gene expression reside at *att*λ as single-copy λ *gnd-lacZ* prophages. The construction of these protein fusions was described previously (5).

The operon fusions CMO69(−) and CMO69(+) were prepared by digesting the plasmids carrying protein fusions CMP69(−) and CMP69(+), respectively, with *Pst*I and *Bam*HI, isolating the *gnd*-containing fragments, and ligating them to the *Bam*HI-*Pst*I fragment of operon fusion vector pMLB1022, which contains the C-terminal coding sequence of *bla*, the plasmid replication origin, and the W205 *′trpA-′lacO-lacZ*$^+$ transcriptional fusion. The recombinant plasmids were introduced into strain HB301 (Δ*lac*) by transformation, and ampicillin-resistant (Ap^r), Lac^+ clones were selected on lactose MacConkey indicator plates containing 10 μg of ampicillin per ml. The fusions were transferred to phage λ by infecting the plasmid-bearing strains with the fusion rescue vector λ RZ5 and recovering the fusion phages by identifying Lac^+ plaques on a lawn of strain HB301 spread on lactose MacConkey plates, as described previously (5). Phage were purified by several rounds of single-plaque isolation and used to transduce HB301 to Lac^+ Ap^r. Monolysogens were identified by a plaque test with phage λ *c*I *c*17, as described previously (5, 20). The constructs were verified by determining the DNA sequence of the entire region from upstream of the *gnd* promoter to downstream of the *gnd-lacZ* fusion joint, as described below.

The 6- and 9-bp deletions scanning the ICS were constructed by PCR with plasmid pCMP69(+) as the DNA template. In each PCR mutagenesis, the upstream primer was oligonucleotide pBR (5′-GTATCACGAGGCCCT-3′), which anneals to vector DNA sequences just counterclockwise to the *Eco*RI site, while the downstream primer contained the deletion. The 5′ end of each mutant oligonucleotide was complementary to the *Bam*HI site and surrounding nucleotides at the junction between the ICS and codon 8 of *lacZ*, and the 3′ end was complementary to at least 11 nucleotides in *gnd* beyond the deletion endpoint. PCR amplifications were carried out under the standard conditions described below, and the products were purified with the Gene Clean II kit of BIO 101 (La Jolla, Calif.). The purified products from a given PCR were digested with *Eco*RI and *Bam*HI, the mixture was treated again with Gene Clean II, and the purified restriction fragment was cloned into plasmid pMLB1034 that had been cleaved with the same enzymes. As controls, the *gnd*-containing *Eco*RI-*Bam*HI fragments of plasmids pCMP69(−) and pCMP69(+) were also cloned into pMLB1034. This was necessary because pMLB1034 lacks the *Eco*RI site that is normally present in *lacZ*, and the *Eco*RI^0 mutation reduces β-galactosidase activity by about 30% (unpublished data). The plasmids were transformed into strain HB301, and Lac^+ Ap^r clones were isolated. The plasmids carrying the deletions were crossed with phage λ RZ5, and monolysogens of strain HB301 were prepared as described above. Each construction was verified by DNA sequencing.

Growth conditions and assays of β-galactosidase activity. Cells were grown at 37°C in morpholinepropanesulfonic acid (MOPS) minimal medium supplemented with either glucose (4.5 g/liter) or potassium acetate (2 g/liter) under the standard physiological conditions described previously by Wolf et al. (25). β-Galactosidase activities in cells permeabilized by treatment with chloroform and sodium dodecyl sulfate were assayed and expressed in Miller units (12). All specific activity values are the averages of duplicate assays of at least two samples from each of two or more independent cultures. On a given day, the standard deviation of the assays for a particular strain was usually less than 10% of the mean value. Day-to-day variation of the specific activity values for a given strain was sometimes more than 10%, but the ratio of values between strains was nearly constant. The growth rate induction ratio is the specific activity of the enzyme during growth on glucose divided by the specific activity on acetate.

PCR amplification and DNA sequencing. The standard PCR mixture of 100 μl contained 10 mM Tris-HCl (pH 9.0 at 25°C), 50 mM KCl, 1.5 mM $MgCl_2$, 0.1% Triton X-100, 200 μM (each) deoxynucleoside triphosphate (dNTP), 10 ng of input DNA template, 0.2 μM each primer, and 2.5 U of *Taq* DNA polymerase (Promega, Madison, Wis.). After an initial incubation at 95°C for 5 min, 30 cycles of the following incubations were carried out: 95°C for 1 min, 50°C for 1 min, and 72°C for 1 min at a ramp rate of 48°C/min. The mixtures were then extracted with the OilAway reagent of BIO 101.

The DNA sequence of each construct was verified by sequencing the entire region from upstream of the *gnd* promoter to downstream of the *gnd-lacZ* fusion joint. We generated single-stranded DNA for sequencing by a modification of the two-stage PCR method of Kaltenboeck et al. (8). A single colony of the construct to be sequenced was resuspended in 50 μl of distilled water, and 5 μl was used as the source of DNA for the first round of PCR. The upstream primer was oligonucleotide pBR, and the downstream primer was oligonucleotide Q4 (5′-CGGGCCTCTTCGCTA-3′), which anneals to the region of *lacZ* between

codons 34 and 29. The second round of PCR contained only the upstream pBR primer. The mixture was subjected to 17 cycles of 95°C for 1 min, 50°C for 1 min, and 72°C for 2 min at a ramp rate of 10°C/min. The single-stranded product from the second round of PCR was purified on a Centricon-30 unit (Amicon, Beverly, Mass.) and sequenced by the chain termination method with Sequenase version 2.0 (United States Biochemicals, Cleveland, Ohio). The DNA sequence across the fusion joint and toward the beginning of the *gnd* structural gene was determined with the −40 universal primer (5′-GTTTTCCCAGTCACGAC-3′), which anneals to codons 17 to 12 of *lacZ*, and the DNA sequence of the *gnd* leader and promoter regions was determined with primer Q3 (5′-CTCACGGGAACGG TTG-3′), which anneals to codons 37 to 32 of *gnd*.

Double-stranded DNA fragments to be used as templates for the T7 RNA polymerase-mediated in vitro transcription of *gnd-lacZ* fusion mRNAs were prepared by PCR under standard conditions, with plasmids carrying the various *gnd-lacZ* protein fusions as input DNA. For these reactions, the downstream primer was oligonucleotide Q4 and the upstream primer was oligonucleotide T7-*gnd* (5′-CCGGAATTCCTAATACGACTCACTATAGAACATTCCAGGC CGCGAGC-3′), which was designed so that the 5′ end of the mRNA transcribed from the PCR product by the T7 RNA polymerase would be identical to the 5′ end of in vivo *gnd* mRNA (15). The PCR product was subjected to agarose gel electrophoresis and eluted from the gel by electroelution. The DNA was further purified by successive extractions with phenol-chloroform and chloroform, and then the DNA was precipitated. The pellet was resuspended in water, and the entire product from a given PCR was used as the DNA template for in vitro transcription with T7 RNA polymerase, as described below.

In vitro transcription. The *gnd-lacZ* fusion mRNAs used in the primer extension inhibition (toeprint) assays and for structural analysis were prepared by in vitro transcription of linear DNA templates with T7 RNA polymerase. The PCR strategy described above was used to replace the native *gnd* promoter with the promoter for T7 RNA polymerase, thereby generating double-stranded DNA templates that could be transcribed by the phage polymerase. In addition to DNA, which was the entire product of a standard PCR, the 100 μl in vitro transcription reaction mixture contained 40 mM Tris-HCl (pH 7.9), 6 mM $MgCl_2$, 2 mM spermidine, 30 mM dithiothreitol, 0.4 mM (each) ribonucleoside triphosphate, RNasin (Promega), and 75 U of T7 RNA polymerase (New England Biolabs, Beverly, Mass.). The mixture was incubated at 37°C for 2 h, after which 10 U of RQ DNase I (Promega) was added and incubation was continued for an additional 20 min. mRNA was extracted successively with phenol-chloroform and chloroform and precipitated with ethanol. The mRNA precipitate was washed with 70% (vol/vol) ethanol, briefly recentrifuged, dried, and resuspended in water. Then residual nucleotides were removed from mRNA by centrifugation on a Microcon-100 unit (Amicon) or by chromatography on a NENsorb (New England Nuclear, Boston, Mass.) column. RNA concentrations were calculated from the A_{260}, assuming that an RNA solution at 40 μg/ml has an absorbance of 1.

Primer extension inhibition (toeprint) assays. Ribosomal 30S subunits were prepared from *E. coli* MRE600 (Grain Processing, Muscatine, Iowa) according to the method of Kenney et al. (10) with some modifications (6). After three rounds of sucrose gradient centrifugation, the purified 30S ribosomal subunits were collected by centrifugation, and the pellet was dissolved in SB buffer (10 mM Tris-acetate [pH 7.4], 60 mM NH_4Cl, 10 mM magnesium acetate, 6 mM β-mercaptoethanol) at as high a concentration as possible. Subunit solutions were stored in several portions at −80°C, and they retained their activities for more than a year.

Formation of the translation initiation complex composed of a 30S ribosomal subunit, a target mRNA, and $tRNA_f^{Met}$ may be detected by the toeprint assay of Hartz et al. (7). A proper concentration of 30S ribosomal subunits was prepared in the SB buffer described above, and the subunits were reactivated prior to use by incubation at 37°C for 15 min (27). Oligonucleotide Q3, complementary to positions 152 to 167 of *gnd* mRNA, was the primer for all assays. mRNAs were synthesized in vitro with T7 RNA polymerase as described above, with DNA templates prepared by PCR.

The mixture for primer-template annealing contained 135 nM mRNA, 810 nM ^{32}P end-labeled DNA primer, and 1 μl of 10× SB without magnesium acetate in a final volume of 10 μl. The annealing mixture was heated to 65°C for 3 min in a heat block and then was cooled slowly to room temperature in the block. Before assay, 2 μl of SB buffer containing 60 mM magnesium acetate was added, which yielded a final Mg^{2+} concentration of 10 mM.

The standard ribosome binding mixture contained 4 μl of annealing mixture, 0.375 mM (each) dNTP, 1.0 μM 30S ribosomal subunits, 10 μM $tRNA_f^{Met}$ (or a threefold molar excess over ribosomes), and 0.5% actinomycin D in a final volume of 9 μl. The final mRNA concentration was 50 nM. Control mixtures lacking the 30S subunits or $tRNA_f^{Met}$ were also prepared. The standard incubation condition for the binding reaction was 37°C for 10 min. After the addition of 2 to 4 U of avian myeloblastosis virus reverse transcriptase (Promega), cDNA synthesis was carried out at 42°C for 10 min. Nucleic acids were precipitated with ethanol, pelleted, rinsed with 70% ethanol, and resuspended in 10 μl of sequencing loading buffer. The sample was heated to 85°C for 3 min prior to electrophoresis on 8% polyacrylamide–50% urea sequencing gels. The position of the toeprint relative to a sequencing ladder was calibrated by using the same end-labeled Q3 primer.

The primer extension products were quantitated with a Molecular Dynamics PhosphorImager model SF (Sunnyvale, Calif.). Signal volumes, which are equivalent to counts per minute per band area, were determined for full-length and extension-inhibited (toeprint) cDNAs. Background signal volumes, which were determined from several areas of the lane, were small and hence ignored. Each relative toeprint value reported as %TP is the toeprint signal volume divided by the sum of the full-length and toeprint volumes times 100. Since the %TP value is a ratio, it is independent of sample recovery and other potential sources of error. Thus, for experiments determining ternary complex formation as a function of the concentration of 30S ribosomal subunits, duplicate samples and even experiments carried out on different days generally showed less than 10% variation.

In experiments determining the rate of ternary complex formation, a single binding mixture was prepared, 9 μl of the mixture was removed at various incubation times, and cDNA synthesis was initiated by the addition of reverse transcriptase. Control experiments reported by Spedding et al. (21), who used toeprint assay conditions very similar to ours, demonstrated that the toeprint signal generated by reverse transcriptase has achieved its half-maximal value by about 1 min.

In vitro mapping of the RBS-ICS secondary structure. Dimethyl sulfate (DMS) and 3-ethoxy-1,1-dihydroxy-2-butanone (also called kethoxal [KE]), which react with unpaired ribonucleotides, were used as probes of mRNA secondary structure. Before chemical treatment, a solution of 50 nM RNA in 10 μl of SB buffer without magnesium acetate and containing 1 mM dithiothreitol in place of β-mercaptoethanol was incubated at 65°C for 3 min, and the mRNA was renatured by slow cooling to room temperature. Before chemical treatment, magnesium acetate was added to a final concentration of 10 mM, as in the toeprint assay.

For the DMS reaction, DMS was diluted 10-fold to a concentration of 42 mM and 1 μl was added to 10 μl of mRNA solution. The reaction was carried out for 10 min in a water bath at ambient temperature. The reaction was stopped by adding 15 μl of TME buffer (100 mM Tris-HCl [pH 7.5], 100 mM β-mercaptoethanol, 5 mM EDTA), and the solution was placed on ice. KE (37 mg) was dissolved in 1 ml of 20% ethanol. To modify mRNA with KE, 1 μl of KE solution was added to 10 μl of mRNA solution, and the reaction mixture was incubated at 37°C for 10 min. The reaction was stopped, and the adducts were stabilized by adding 15 μl of 1 M potassium borate [pH 7.0] and setting the mixture on ice.

After chemical treatment, the samples were precipitated with ethanol and washed with 70% ethanol. Modified mRNAs were then annealed to the appropriate primer under the conditions described above for the toeprint assay. Bases modified by DMS and KE can be detected as stops in cDNA synthesis carried out by reverse transcription. Thus, reverse transcription reaction mixtures were prepared by adding 2 to 4 U of avian myeloblastosis virus reverse transcriptase, 1 μl of actinomycin D, and 0.375 mM dNTPs to the solution of modified RNA, and the mixtures were incubated at 42°C for 15 min. cDNA synthesis was then stopped by ethanol precipitation, and the pellet was dissolved in 5 μl of loading buffer. After denaturation, samples were subjected to gel electrophoresis and autoradiography. The codon 8 primer (5′-CCCATCACTGCCATACC-3′), which anneals to positions 44 to 28 of the 6PGD coding sequence, was used to detect the modified bases of the *gnd* mRNA leader. The primer for detecting the modified bases of the ICS was the −50 primer (5′-TAACGCCAGGGTTTTC-3′), which anneals to codons 22 to 17 of *lacZ*.

RESULTS

Differing effects of the ICS in protein and operon fusions. As a means of assessing whether the ICS is a transcriptional operator or attenuator rather than a posttranscriptional regulator, we compared the effects of the ICS in operon and protein fusions. The fusions were crossed on to phage λ, and the resulting fusion phages were integrated in single copy at *att*λ, the manner in which most previous genetic analyses had been done (5). The fusions had the same amount of upstream *gnd* DNA, extending to position −135 with respect to the transcription initiation site, and 69 *gnd* codons were fused to *lacZ* or *′lacO*; they differed with respect to the absence or presence of the 16-bp core ICS element (5). Since the negative effect of the ICS in *gnd-lacZ* protein fusions is greater under slow-growth conditions than under fast-growth conditions, the β-galactosidase activities in cultures of fusion strains growing exponentially in acetate and glucose minimal media were determined.

Table 1 compares the effects of the ICS on β-galactosidase production in strains carrying *gnd-lacZ* protein fusions to those of strains carrying *gnd-lac* operon fusions. As reported previously for protein fusions at *att*λ (5), the presence of the ICS reduces β-galactosidase activity 4- to 5-fold during growth on

TABLE 1. Differing effects of the ICS on growth rate-dependent regulation of the β-galactosidase level in *gnd-lac* operon and protein fusion strains

Strain	β-Galactosidase (Miller units) during growth on:		Induction ratio
	Acetate	Glucose	
CMP69(−)	3,454	2,076	0.6
CMP69(+)	816	920	1.1
ICS^-/ICS^+ ratio	4.2	2.3	
CMO69(−)	4,340	3,101	0.7
CMO69(+)	3,314	2,761	0.8
ICS^-/ICS^+ ratio	1.3	1.1	

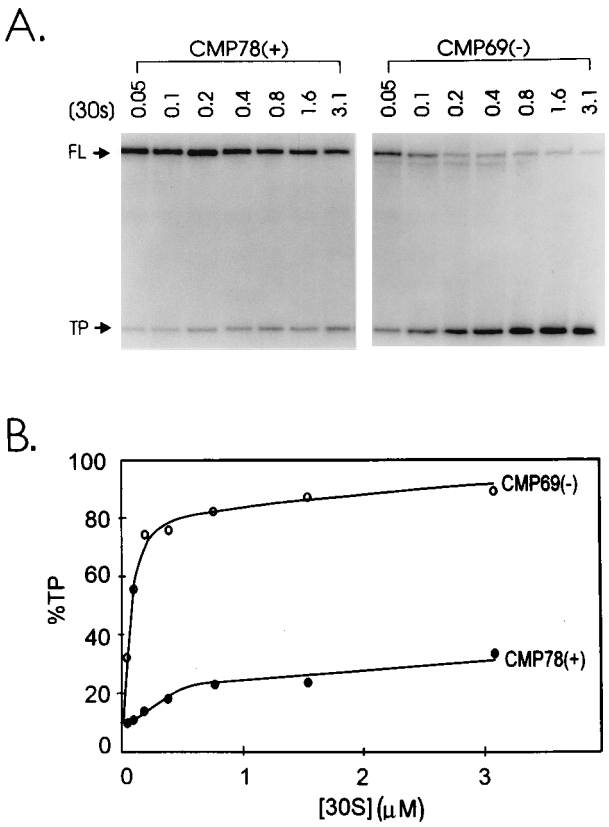

FIG. 1. The dependence of ternary complex formation on the concentration of 30S ribosomal subunits with CMP69(−) and CMP78(+) fusion mRNAs. Increasing concentrations of purified 30S ribosomal subunits were incubated at 37°C for 10 min with 50 nM fusion mRNA and 10 μM $tRNA_f^{Met}$-mRNA, and then cDNA synthesis was carried out with avian myeloblastosis virus reverse transcriptase. (A) Autoradiogram of the products of cDNA synthesis after electrophoresis on a sequencing gel. The toeprint (TP) signal is at +14, with the first base of the coding sequence numbered as 0, and the full-length (FL) signal corresponds to the 5′ end of the mRNA. A weak reverse transcriptase stop is at position −32U (see Fig. 4, left), which lies at the 3′ end of a GC-rich stem-loop structure in the *gnd* mRNA leader (4, 6). (B) The TP and FL signals were quantified with a PhosphorImager, and the %TP values, calculated as the TP signal divided by the sum of the TP and FL signals times 100, were plotted as a function of the concentration of 30S ribosomal subunits.

acetate and about 2.5-fold during growth on glucose [compare the results for CMP69(+) with those for CMP69(−)]. In contrast, the ICS has little or no effect on β-galactosidase production in the companion operon fusion strains [compare the results for CMO69(+) with those for CMO69(−)]. These results suggest that the ICS does not function as a transcriptional operator or attenuator. They also suggest that the ICS is probably not a site for growth rate-dependent endonucleolytic cleavage of *gnd* mRNA, for if it were, its presence in an operon fusion would likely reduce β-galactosidase expression.

Effect of the ICS on the binding of 30S ribosomal subunits to *gnd* mRNA in vitro. To test directly whether the ICS negatively regulates translation initiation, we used the primer extension inhibition (toeprint) assay (7) to quantitate the amounts of the translation initiation (ternary) complex formed on *gnd*-lacZ protein fusion mRNAs containing or lacking the ICS. In the standard toeprint assay, ternary complexes composed of mRNA, $tRNA_f^{Met}$, and 30S ribosomal subunits purified as described in Materials and Methods are formed at 37°C for 10 min and then reverse transcriptase and dNTPs are added to initiate cDNA synthesis from an end-labeled primer previously hybridized to mRNA at a site downstream of the RBS. The ternary complex is stable enough that primer extension by reverse transcriptase is blocked at the 3′ edge of the bound 30S subunit, and thus a truncated cDNA (toeprint) product is produced. Full-length (i.e., unblocked) and truncated extension products are then separated on a sequencing gel, and the resulting signals are quantitated. With *gnd* mRNA, the reverse transcriptase stop is at +14, with the first nucleotide of the start codon numbered as 0 (data not shown).

Under the standard reaction conditions (37°C, 10 min), the %TP of the ICS^- mRNA CMP69(−) increases with an increasing concentration of the 30S ribosomal subunits until maximum binding is achieved at 1 μM subunits (Fig. 1). Similar to the in vivo effect of the ICS on gene expression, in which the regulatory element reduces β-galactosidase synthesis by 2.5- to 5-fold, the presence of the ICS in CMP78(+) mRNA reduces the maximum binding of the 30S ribosomal subunits in vitro by 3-fold (Fig. 1). Thus, these in vitro ribosome binding assays clearly demonstrate that the presence of the ICS in *gnd-lacZ* mRNA inhibits formation of the translation initiation complex. Importantly, since no other cellular components, like mRNA-binding proteins, are present in the binding assay, these data further suggest that the ability of the putative long-range RBS-ICS secondary structure to form and inhibit translation initiation does not require other cellular factors that could affect the rate or the stability of secondary structure formation.

Since formation of the pretranslation initiation complex is irreversible (18, 19, 21), the presence of the ICS should reduce the rate of ternary complex formation by the same factor with which it reduces the maximum extent of ribosome binding. Accordingly, we mixed 30S ribosomal subunits at a concentration of 0.1 μM with 1 μM $tRNA_f^{Met}$ and either ICS^- or ICS^+ mRNA at 50 nM, incubated the components at 37°C, and measured the kinetics of ternary complex formation by adding reverse transcriptase and dNTPs to samples taken at various times. The initial rate of forming the ternary complex on CMP69(−) mRNA was 5.7%TP per min, about 3.3-fold higher than the rate (1.9%TP per min) of complex formation on CMP78(+) mRNA (Fig. 2). Thus, the presence of the ICS reduces both the initial rate of and the maximum amount of ternary complex formation.

We also carried out toeprint assays under standard conditions with CMP40(+) and CMP69(+) fusion mRNAs (data not shown), which have single copies of the ICS at codons 40 and 69, respectively, and which produce the same amount of β-galactosidase in vivo as does CMP78(+) (5). The %TP values were 19 and 9, respectively. In the same set of experiments,

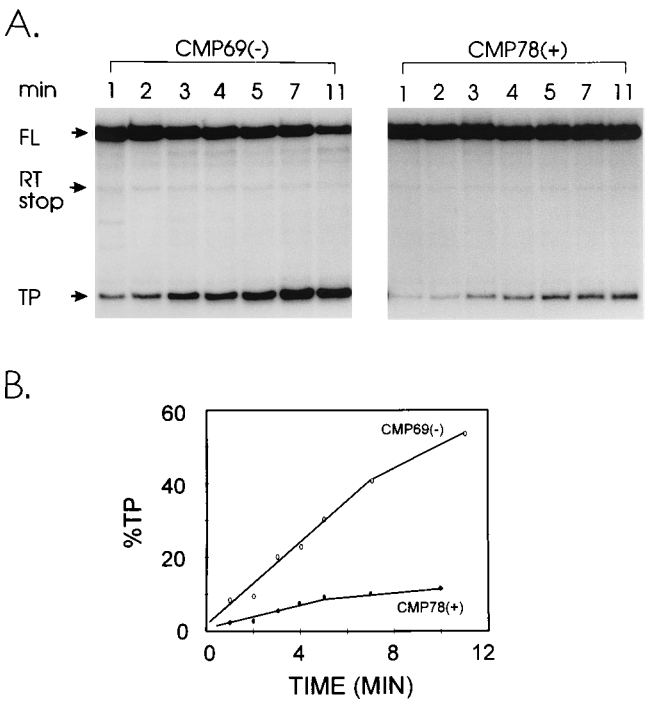

FIG. 2. The effect of the ICS on the rate of ternary complex formation. (A) CMP69(−) and CMP78(+) fusion mRNAs were incubated at 37°C with 0.1 μM 30S ribosomal subunits and 0.3 μM $tRNA_f^{Met}$ for the indicated times before the reaction was terminated and cDNA synthesis was initiated by the addition of reverse transcriptase (RT). TP, toeprint signal; FL, full-length signal. (B) The RT products were quantified with a PhosphorImager, and the %TP values were plotted as a function of time. The apparent initial rate of ternary complex formation was 5.7%TP per min on the ICS^- mRNA and 1.9%TP per min on the ICS^+ mRNA.

the %TP values for mRNAs CMP69(−) and CMP78(+) were 68 and 20, respectively.

Effects of small deletions scanning the ICS on gene expression in vivo and ribosome binding in vitro. As a way of potentially identifying domains of the ICS to be subjected to base substitution mutagenesis, we prepared all possible 6- and 9-bp deletions across the core ICS element of protein fusion CMP69(+) and determined their effects on gene expression in vivo and on ribosome binding in vitro. The deletions scanning the ICS element were prepared by synthesizing oligonucleotides containing the desired deletions and then using PCR to introduce the respective deletions into DNA fragments of CMP69(+) that were subsequently cloned into the protein fusion vector pMLB1034. We then transferred each mutant fusion to phage λ, prepared single-copy lysogens of the mutant phages, and measured the β-galactosidase activities in lysogens during exponential growth in glucose minimal medium. We also prepared fusion mRNAs containing the respective deletions and determined the maximum extent of ternary complex formation on each mRNA. The deletions conferred a spectrum of phenotypes, with some completely eliminating ICS function and others being silent or conferring an intermediate phenotype (Table 2). Importantly, the effects of the respective deletions on gene expression in vivo were highly correlated with the effects on ribosome binding in vitro: the correlation coefficient of the linear regression line relating the two parameters was 0.92. Thus, since the in vivo effects on gene expression of the deletions scanning the ICS can be fully accounted for by corresponding effects on ribosome binding in vitro, we infer that the primary in vivo function of the ICS is to reduce the frequency of translation initiation.

Effect of the presence of the ICS on the single strandedness of the *gnd* RBS. Since the data obtained with the toeprint assay are consistent with the hypothesis that an RBS-ICS secondary structure forms in vitro, we probed the in vitro structure of *gnd* mRNA with the single-strand-specific reagents DMS and KE. Modifications of A and C by DMS and of G by KE interfere with cDNA synthesis by reverse transcriptase and cause reverse transcriptase to stop one residue before the modified base. Rather than determining the complete structure of *gnd* mRNA from its 5′ end to beyond the ICS, we investigated whether the presence of the ICS in an mRNA reduces the susceptibility of the RBS to attack by these single-strand-specific chemical reagents. We used the codon 8 primer of the *gnd* gene to detect modified bases in the RBS and the −50 forward primer of the *lacZ* gene (described in Materials and Methods) to probe the ICS region. Mapping was done with the same *gnd-lacZ* fusion mRNAs and under the same conditions used in the toeprint experiments.

We first subjected ICS^- mRNAs to treatment with DMS and KE. With CMP40(−) (Fig. 3A) and CMP69(−) (data not shown), the entire RBS region from G-33 to G-59, which includes the Shine-Dalgarno sequence and the AUG start codon, was attacked by the single-strand-specific chemical probes. On the other hand, the Shine-Dalgarno sequence and the adjacent bases on the upstream side were protected from

TABLE 2. Correlation between gene expression in vivo and ribosome binding in vitro in a set of deletions scanning the ICS

Strain	DNA sequence of the ICS region			%TP	β-Galactosidase (Miller units)
	Codons 68–71	Core ICS element	Fusion joint		
CMP69(−)	CGTCCGGATCT	---------------	GGATCCCGTCGT	65	1,572
CMP69(+)	CGTCCGGATCT	CATCCTGTTAATGGT	GGATCCCGTCGT	10	505
6-bp deletions					
CMP69(+)D15	CGTCCGGATCT	------GTTAATGGT	GGATCCCGTCGT	10	245
CMP69(+)D1	CGTCCGGATCT	C------TTAATGGT	GGATCCCGTCGT	20	500
CMP69(+)D16	CGTCCGGATCT	CA------TAATGGT	GGATCCCGTCGT	30	466
CMP69(+)D18	CGTCCGGATCT	CATC------ATGGT	GGATCCCGTCGT	32	756
CMP69(+)D9	CGTCCGGATCT	CATCC------TGGT	GGATCCCGTCGT	33	766
CMP69(+)D8	CGTCCGGATCT	CATCCTGTT------	GGATCCCGTCGT	36	655
9-bp deletions					
CMP69(+)D11	CGTCCGGATCT	---------AATGGT	GGATCCCGTCGT	28	784
CMP69(+)D5	CGTCCGGATCT	C---------ATGGT	GGATCCCGTCGT	27	973
CMP69(+)D13	CGTCCGGATCT	CATC---------GT	GGATCCCGTCGT	58	1,436
CMP69(+)D14	CGTCCGGATCT	CATCCT---------	GGATCCCGTCGT	56	1,300

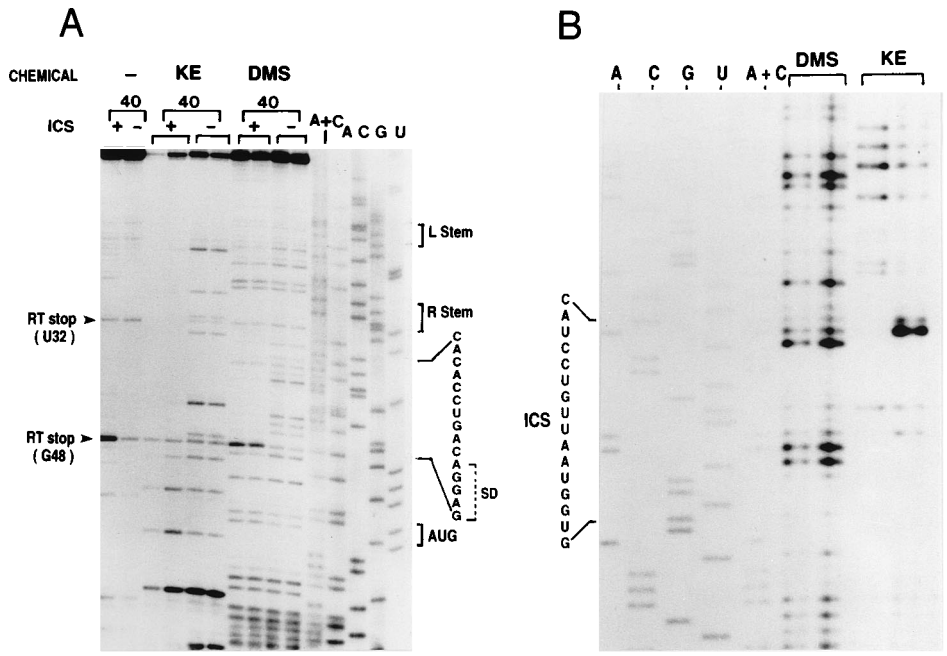

FIG. 3. Autoradiogram of the structure mapping of fusion mRNAs CMP40(−) and CMP40(+). mRNAs were treated with either DMS or KE for 10 min at 18 or 37°C, respectively. The reactions were stopped by the addition of the appropriate stop solution, and each treated mRNA was divided into two parts. One part was annealed with the codon 8 primer for the detection of modified bases in the RBS (A); the other part was annealed with the −50 forward primer for the detection of modified bases in the ICS (B). The sequence ladders (lanes A, C, G, U, and A+C) were generated by the respective primers on DNA templates. Note that cDNA synthesis stops one residue before the modified base. Reverse transcriptase (RT) stops other than those due to base modifications were produced at positions U-32 and G-49 in the *gnd* mRNA leader. The stop at position U-32 is at the 3′ end of the leader's GC-rich stem-loop structure.

attack by DMS and KE in the ICS$^+$ mRNAs CMP40(+) (Fig. 3A) and CMP69(+) (data not shown); moreover, the ICS of these mRNAs was not modified by either reagent (Fig. 3B). These results, which are summarized in Fig. 4, show that the presence of the ICS in CMP40(+) and CMP69(+) prevents chemical attack of the RBS, and presumably it is the RBS that blocks attack of the ICS. The inference drawn from these data is that the complementary bases of the RBS and the ICS directly pair with one another in a long-range RBS-ICS structure, although the possibility that the effect of the ICS is indirect has not been ruled out.

We also probed the structure of ICS$^+$ mRNA CMP78(+) (summarized in Fig. 4). With this mRNA, the 5′ end of the RBS (5′ [38]-CACC-3′) was partially protected from DMS modification, while its putative complement, the 3′ end of the ICS (5′ [275]-GGUG-3′), was sensitive to the reagent. The 3′ end of the RBS (5′ [46]-AGGA-3′) in the ICS$^+$ mRNA was modified by DMS, but its complement, the 5′ end of the ICS (5′ [265]-UCCU-3′), was protected from attack by the reagent.

DISCUSSION

The work presented here has consolidated our view of the growth rate-dependent regulation of the *E. coli gnd* gene. Previous research had indicated that the amount of 6PGD mass increases with an increasing growth rate (25), that a posttranscriptional step in *gnd* expression is probably subject to growth rate-dependent control (1), and that regulation of the 6PGD level involves the ICS, a negative control site in the *gnd* structural gene whose mRNA sequence is complementary to the RBS of the *gnd* mRNA leader (2, 5). Although reasonable models integrating these facts have been proposed (4, 5), important gaps between interpretation and experimental verification remained.

A basic question that needed to be addressed was whether the posttranscriptional regulation inferred from the properties of *gnd-lac* operon fusions (1) involved the ICS, whose role in growth rate-dependent regulation was revealed by *gnd-lacZ* protein fusions containing or lacking the element (2, 5). The data presented in Table 1 rule out the possibility that the ICS is a site of growth rate-dependent transcriptional repression or attenuation by showing directly that the ICS affects gene expression only in protein fusions, not in operon fusions.

The work described here is consistent with the primary role of the ICS being to regulate translation efficiency through the regulation of translation initiation. Toeprint assays demonstrated that the presence of the ICS in *gnd* mRNA reduces both the maximum extent and the rate of formation of the translation preinitiation ternary complex by a factor similar to the effect of the ICS on gene expression in vivo (Fig. 1 and 2). Moreover, the effects of deletions scanning the ICS on the extent of 30S ribosome binding in vitro were highly correlated with the effects of the deletions on in vivo gene expression. This correlation suggests that the inhibition of translation initiation may be the sole regulatory role of the ICS.

To address the hypothesis that the ICS regulates translation initiation by sequestering the RBS into an RBS-ICS secondary structure, we determined whether the presence of the ICS in *gnd* mRNA reduces the susceptibility of the RBS to attack by single-strand-specific chemical reagents (compared with ICS$^-$ mRNA). We found that whereas the entire RBS is susceptible to attack in ICS$^-$ mRNAs CMP40(−) and CMP69(−), it is attacked less or not at all in ICS$^+$ mRNAs CMP40(+) and CMP69(+) and the ICS itself is only weakly attacked (Fig. 3 and 4). Thus, these results are consistent with the essential feature of the model, which is that the ICS leads to the formation of a secondary structure that blocks the access of the

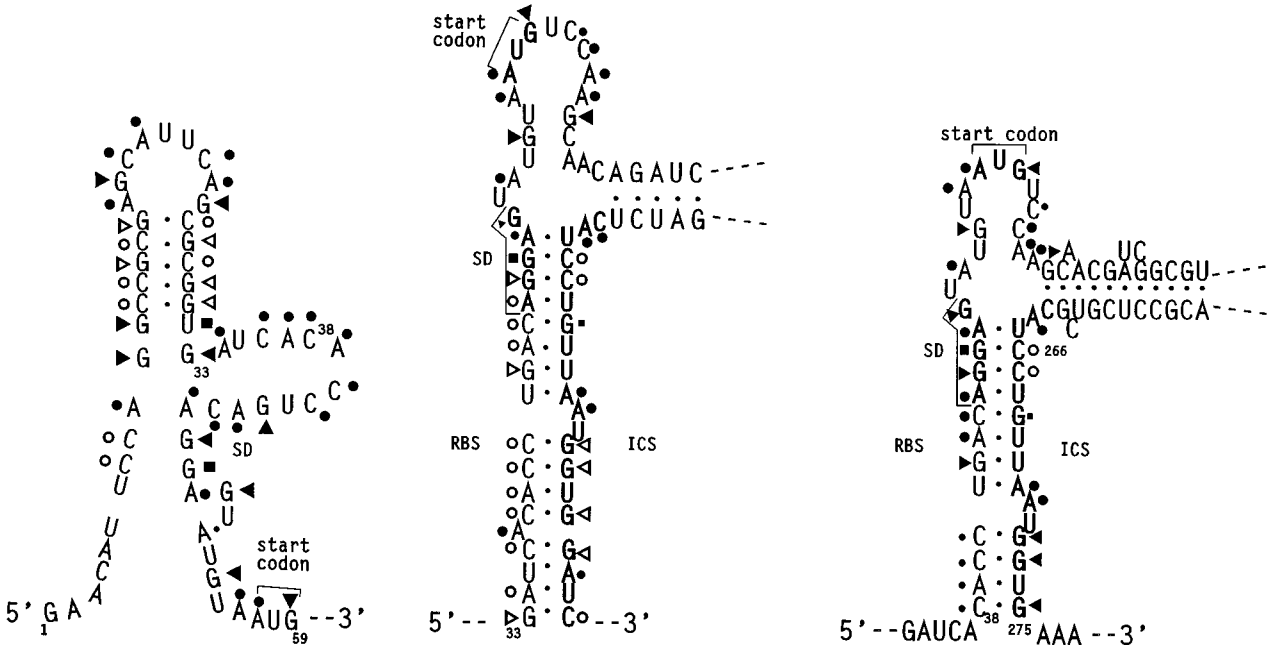

FIG. 4. Summary of the structure mapping of ICS$^-$ and ICS$^+$ mRNAs. Fusion mRNAs CMP40(−), CMP69(−), CMP40(+), and CMP69(+) were probed with the single-strand-specific chemical reagents DMS and KE (Fig. 3 and data not shown). Emphasis was placed on comparing modifications of the RBS region in ICS$^+$ mRNAs with those in ICS$^-$ mRNAs. Solid circles indicate bases modified by DMS, solid triangles indicate bases modified by KE, solid squares indicate sites at which reverse transcriptase stops on unmodified DNA, and smaller symbols indicate weaker modification signals. Open symbols designate residues not attacked by the reagents. (Left) Summary of the structure probing of the leader of CMP40(−) mRNA, as shown in Fig. 3, and that of CMP69(−) (data not shown). (Center) Summary of the structure probing of CMP40(+) fusion mRNA, as shown in Fig. 3, and that of CMP69(+) (data not shown). The structure shown is the most stable secondary structure of the fusion mRNA extending from its 5′ end to codon 35 of *lacZ*, as predicted by the MFold program of the Genetics Computer Group package of computer software. Note that the sequence of CMP69(+) is exactly the same as that of CMP40(+) for the residues shown. (Right) Summary of the structure probing of CMP78(+) fusion mRNA (data not shown). The structure shown is the most stable secondary structure of *gnd* mRNA from its 5′ end to codon 78, as predicted by the MFold program. SD, Shine-Dalgarno sequence.

30S ribosomal subunit to the RBS, although they do not prove that the two mRNA elements are protected from attack because they are directly base paired to one another. In other words, rather than directly pairing with the RBS, the ICS might pair with one arm of a noninhibitory hairpin that is present in ICS$^-$ mRNA, thereby allowing the other arm to pair with and sequester the RBS. However, computer analysis of the potential secondary structures of ICS$^-$ and ICS$^+$ *gnd* mRNAs did not reveal such alternative foldings.

We are not sure why the susceptibility of the RBS and the ICS of CMP78(+) mRNA to attack by single-strand-specific chemical reagents differs from those of CMP40(+) and CMP69(+) mRNAs (Fig. 4). On the one hand, it might be that the RBS and the ICS are base paired directly in CMP40(+) and CMP69(+) but only indirectly in CMP78(+). Alternatively, the RBS-ICS structure might exist in all three mRNAs, but the stability of the structure in CMP78(+) might be less than the stabilities of the CMP40(+) and CMP69(+) mRNAs. Indeed, the MFold program of the Genetics Computer Group package of computer software predicted that the fraction of CMP78(+) molecules in which the RBS is base paired with the ICS is much smaller than those of CMP40(+) and CMP69(+) mRNAs. Moreover, it may be unreasonable to expect that the presence of the ICS would completely block attack of the RBS by these chemical reagents, even if the model is correct that the ICS functions by directly sequestering the RBS into a secondary structure. First, DMS and KE are small molecules that would attack residues in a paired structure should any breathing (opening and closing) of the structure occur. In this regard, the differences between the mRNAs may be only quantitative and may be due to small differences in reaction conditions, e.g., the concentration of mRNA subjected to chemical treatment. Second, regardless of whether structure breathing actually occurs, the toeprint assays of the ICS$^+$ mRNAs showed that in about 20% of molecules, the RBS is able to be bound by 30S ribosomal subunits. Thus, at a minimum, the RBS region of a similar fraction of molecules should be attackable by single-strand-specific reagents.

As a means of identifying the region(s) of the ICS most critical to its regulatory function, we prepared a set of all possible 6- and 9-bp deletions across the ICS. A close examination of the data presented in Table 2 reveals a striking pattern. As the deletions scan across the ICS in the 5′-to-3′ direction, the extent of in vitro 30S binding increases, i.e., the inhibitory effect of the ICS on translation initiation decreases. Thus, with the 6-bp deletions, the %TP values are 10, 20, 30, 32, 33, and 36 for deletions D15, D1, D16, D18, D9, and D8, respectively; with the 9-bp deletions D11, D5, D13, and D14, the %TP values are 28, 27, 58, and 56, respectively. Apparently, the proximal segment of the ICS (5′-CATCCT-3′), which contains the anti-Shine-Dalgarno sequence, is less important to the formation of the putative long-range RBS-ICS secondary structure and hence to ICS function than is the distal segment (5′-ATGGT-3′); thus, the ICS is completely nonfunctional, 56%TP, in deletion D14, which retains the sequence 5′-CATCCT-3′, while it functions at an intermediate level, 28%TP, in deletion D11, which retains the sequence 5′-AATGGT-3′. Moreover, this analysis also indicates that the G and T residues immediately downstream of the TCCT anti-Shine-Dalgarno sequence, which are successively removed by deletions D1 and D16, play a critical role in ICS function; the extent of ternary complex formation increases in two 10%TP

increments as the 6-bp deletion window scans from D15 to D1 to D16. A similar conclusion may be reached by comparing the effect of the 9-bp deletion D14, which retains only the 5′-CATCCT-3′ sequence of the ICS, with that of the 6-bp deletion D8, which retains the 5′-CATCTTGTT-3′ segment. The %TP value for D14 is 56%, while the %TP value for D8 is 36%. In summary, the pattern of the effects of deletions on ternary complex formation in vitro will guide us in choosing specific nucleotides as targets for further site-directed mutagenesis. Specifically, the analysis described above suggests that genetic proof for the in vivo formation of the RBS-ICS secondary structure might best be obtained by the isolation of double- or triple-base substitution mutations in the distal segment of the ICS combined with the isolation of the corresponding compensatory mutations of the RBS.

The literature now contains a number of examples of regulatory elements that seem to function by the formation of a long-range secondary structure that blocks translation initiation. These translation inhibitors can be divided into two groups, those like the *gnd* ICS that lie in the regulated structural gene and others like the Min Jou sequence of RNA phage MS2 (13) that mediate translational coupling between two genes in the same transcriptional unit. Members of the former group include the gene for the 21-kDa protein in the *trmD* operon (23, 24) and the genes for the heat shock (9, 14, 26) and stationary-phase (11) sigma factors of RNA polymerase, while members of the latter group include the *rplJL* ribosomal protein genes (17) and the coat protein-replicase genes of phage MS2 (22). Although the advantage of this form of regulation is not yet apparent, it is interesting that most of the genes using it are involved in essential cellular processes, namely, growth or survival to stress. Moreover, although the ability of *gnd*'s ICS element to sequester the RBS does not appear to require a *trans*-acting factor, the analogous elements in the σ^H and σ^S genes almost certainly do.

ACKNOWLEDGMENTS

We thank Penelope Carter-Muenchau for able technical assistance during the early phase of this work, David Draper and Gary Spedding for helpful discussions regarding preparation of 30S ribosomal subunits and toeprint assays, and Michael O'Neill for his continued interest in this research.

This work was supported by NIH grant GM27113.

REFERENCES

1. **Baker, H. V., II, and R. E. Wolf, Jr.** 1983. Growth rate-dependent regulation of 6-phosphogluconate dehydrogenase level in *Escherichia coli* K-12: β-galactosidase expression in *gnd-lac* operon fusion strains. J. Bacteriol. **153:**771–781.
2. **Baker, H. V., II, and R. E. Wolf, Jr.** 1984. Essential site for growth rate-dependent regulation within the *Escherichia coli gnd* structural gene. Proc. Natl. Acad. Sci. USA **81:**7669–7673.
3. **Barcak, G. J., and R. E. Wolf, Jr.** 1988. Growth-rate-dependent expression and cloning of *gnd* alleles from natural isolates of *Escherichia coli*. J. Bacteriol. **170:**365–371.
4. **Barcak, G. J., and R. E. Wolf, Jr.** 1988. Comparative nucleotide sequence analysis of growth-rate-regulated *gnd* alleles from natural isolates of *Escherichia coli* and from *Salmonella typhimurium* LT-2. J. Bacteriol. **170:**372–379.
5. **Carter-Muenchau, P., and R. E. Wolf, Jr.** 1989. Growth-rate-dependent regulation of 6-phosphogluconate dehydrogenase level mediated by an anti-Shine-Dalgarno sequence located within the *Escherichia coli gnd* structural gene. Proc. Natl. Acad. Sci. USA **86:**1138–1142.
6. **Chang, J. T.** 1994. Ph.D. thesis. University of Maryland Baltimore County, Catonsville.
7. **Hartz, D., D. S. McPheeters, R. Traut, and L. Gold.** 1988. Extension inhibition analysis of translation initiation complexes. Methods Enzymol. **164:** 419–425.
8. **Kaltenboeck, B., J. W. Spatfora, X. Zhang, K. G. Kousalas, M. Blockwell, and J. Storz.** 1991. Efficient production of single-stranded DNA as long as 2 kb for sequencing of PCR-amplified DNA. BioTechniques **12:**164–171.
9. **Kamath-Loeb, A. S., and C. A. Gross.** 1991. Translational regulation of σ^{32} synthesis: requirement for an internal control element. J. Bacteriol. **173:** 3904–3906.
10. **Kenney, J. W., T. G. Fanning, J. M. Lambert, and R. R. Traut.** 1979. The subunit interface of the *Escherichia coli* ribosome. J. Mol. Biol. **135:**151–170.
11. **Lange, R., and R. Hengge-Aronis.** 1994. The cellular concentration of the σ^S subunit of RNA polymerase in *Escherichia coli* is controlled at the levels of transcription, translation, and protein stability. Genes Dev. **8:**1600–1612.
12. **Miller, J. H.** 1972. Experiments in molecular genetics. Cold Spring Harbor Laboratory, Cold Spring Harbor, N.Y.
13. **Min Jou, W., G. Haegeman, M. Ysebaert, and W. Fiers.** 1972. Nucleotide sequence of the gene coding for the bacteriophage MS2 coat protein. Nature (London) **237:**82–88.
14. **Nagai, H., H. Yuzawa, and T. Yura.** 1991. Interplay of two cis-acting mRNA regions in translational control of σ^{32} synthesis during the heat shock response of *Escherichia coli*. Proc. Natl. Acad. Sci. USA **88:**10515–10519.
15. **Nasoff, M. S., H. V. Baker II, and R. E. Wolf, Jr.** 1984. DNA sequence of the *Escherichia coli* gene, *gnd*, for 6-phosphogluconate dehydrogenase. Gene **27:**253–264.
16. **Pease, A. J., and R. E. Wolf, Jr.** 1994. Determination of the growth rate-regulated steps in expression of the *Escherichia coli* K-12 *gnd* gene. J. Bacteriol. **176:**115–122.
17. **Petersen, C.** 1992. Long-range translational coupling in the *rplJL-rpoBC* operon of *Escherichia coli*. J. Mol. Biol. **206:**323–332.
18. **Philippe, C., L. Bénard, F. Eyermann, C. Cachia, S. V. Kirillov, C. Portier, B. Ehresmann, and C. Ehresmann.** 1994. Structural elements of *rpsO* mRNA involved in the modulation of translational initiation and regulation of *E. coli* protein S15. Nucleic Acids Res. **22:**2538–2546.
19. **Risuleo, G., C. Gualerzi, and C. Pon.** 1976. Specificity and properties of the destabilization, induced by initiation factor IF-3, of ternary complexes of the 30-S ribosomal subunit, aminoacyl-tRNA and polynucleotides. Eur. J. Biochem. **67:**603–613.
20. **Shimada, K., R. A. Weisberg, and M. E. Gottesman.** 1972. Prophage lambda at unusual chromosomal locations. I. Location of the secondary attachment sites and the properties of the lysogens. J. Mol. Biol. **63:**483–503.
21. **Spedding, G., T. C. Gluick, and D. Draper.** 1993. Ribosome initiation complex formation with the pseudoknotted α operon messenger RNA. J. Mol. Biol. **229:**609–622.
22. **van Himbergen, J., B. van Geffen, and J. van Duin.** 1993. Translational control by a long range RNA-RNA interaction: a basepair substitution analysis. Nucleic Acids Res. **21:**1713–1717.
23. **Wikström, P. M., and G. R. Björk.** 1989. A regulatory element within a gene of a ribosomal protein operon of *Escherichia coli* negatively controls expression by decreasing the translational efficiency. Mol. Gen. Genet. **219:**381–389.
24. **Wikström, P. M., L. K. Lind, D. E. Berg, and G. R. Björk.** 1992. Importance of mRNA folding and start codon accessibility in the expression of a gene in a ribosomal protein operon of *Escherichia coli*. J. Mol. Biol. **224:**949–966.
25. **Wolf, R. E., Jr., D. M. Prather, and F. M. Shea.** 1979. Growth-rate-dependent alteration of 6-phosphogluconate dehydrogenase and glucose 6-phosphate dehydrogenase levels in *Escherichia coli* K-12. J. Bacteriol. **139:**1093–1096.
26. **Yuzawa, H., H. Nagai, H. Mori, and Y. Yura.** 1993. Heat induction of σ^{32} synthesis mediated by mRNA secondary structure: a primary step of the heat shock response in *Escherichia coli*. Nucleic Acids Res. **21:**5449–5455.
27. **Zamir, A., R. Miskin, and D. Elson.** 1971. Inactivation and reactivation of ribosomal subunits: amino acyl-transfer RNA binding activity of the 30S subunit of *Escherichia coli*. J. Mol. Biol. **60:**347–364.